

MINERALOGY

Discovery of davemaoite, CaSiO₃-perovskite, as a mineral from the lower mantle

Oliver Tschauner^{1*}, Shichun Huang¹, Shuying Yang², Munir Humayun², Wenjun Liu³, Stephanie N. Gilbert Corder⁴, Hans A. Bechtel⁴, Jon Tischler³, George R. Rossman⁵

Calcium silicate perovskite, CaSiO₃, is arguably the most geochemically important phase in the lower mantle, because it concentrates elements that are incompatible in the upper mantle, including the heat-generating elements thorium and uranium, which have half-lives longer than the geologic history of Earth. We report CaSiO₃-perovskite as an approved mineral (IMA2020-012a) with the name davemaoite. The natural specimen of davemaoite proves the existence of compositional heterogeneity within the lower mantle. Our observations indicate that davemaoite also hosts potassium in addition to uranium and thorium in its structure. Hence, the regional and global abundances of davemaoite influence the heat budget of the deep mantle, where the mineral is thermodynamically stable.

Calcium silicate, CaSiO₃, occurs in a variety of natural and synthetic polymorphs. The low-pressure polymorph wollastonite is a common metamorphic mineral. Breyite (1), an intermediate-pressure polymorph (2), has been found as inclusions in diamond. At the pressures and depth range of Earth's transition zone (420 to 660 km) and lower mantle (LM; 660 to ~2700 km), CaSiO₃ assumes a perovskite structure. Perovskite-type CaSiO₃, first synthesized by Liu and Ringwood (3), is a liquidus phase for basaltic and peridotite bulk rock compositions at LM pressures and temperatures and has been experimentally shown to host many elements that are incompatible in upper-mantle minerals (4–7). These include rare-earth elements (REEs), large ion lithophile elements (LILEs; K, Sr, and Ba), Ti, U, and Th. In other words, these elements are compatible rather than incompatible in a LM mineral assemblage that contains a few vol % of CaSiO₃-perovskite. The composition and abundance of this phase in the LM are therefore key in constraining the budget and distribution of REEs and LILEs and the elements with abundant radioactive isotopes (K, U, and Th) that make an important contribution to the heat of Earth's mantle (8). Through these parameters, CaSiO₃ perovskite provides essential constraints on the fate of recycled crust in deep Earth, thermochemical anomalies, and the existence of a magma ocean at the base of Earth's mantle. The synthetic perovskite phase of pure CaSiO₃ has been found to assume either cubic or tetragonal symmetry (9) and belongs to the tausonite (SrTiO₃)-type perovskites that

adhere to fundamentally different structural distortion mechanisms (10) and crystal-chemical constraints than the GdFeO₃-type perovskites such as bridgmanite [MgSiO₃-perovskite (11)] and the CaTiO₃ mineral, actually named perovskite.

The difficulty of finding CaSiO₃-perovskite in nature stems from its stability at pressures only above 20 GPa (3, 4) along with a low kinetic barrier for back-conversion into low-pressure polymorphs (2). This barrier is lower than for bridgmanite, which has been found as a rare occurrence in highly shocked meteorites despite its stability only above 23 GPa (11, 12). Nestola *et al.* (13) reported the presence of CaSiO₃-perovskite as an inclusion in a diamond from the Cullinan mine, South Africa. The reported phase deviates from synthetic CaSiO₃-perovskite in several ways: (i) its volume at ambient conditions is >20% larger (9); (ii) it sustains the beam of an electron microscope, whereas any synthetic CaSiO₃-perovskite vitrifies rapidly at ambient conditions; (iii) its cell axis ratios and Raman spectrum are nearly equal to those of CaTiO₃; and (iv) its space group indicates a structural distortion mechanism different from that of synthetic CaSiO₃-perovskite but much closer to that of CaTiO₃ (7, 8). Nestola *et al.* (13) proposed that this distinctive phase of CaSiO₃ is the result of partial decomposition of a Ti-bearing CaSiO₃-perovskite. The coexistence of CaTiO₃ + CaSiO₃ polymorphs in diamond inclusions may also point to retrograde transformation of stoichiometric Ca-Si-Ti-perovskites (1) that form in the deep upper mantle (5 to 10 GPa).

The findings by Nestola *et al.* (13) are notable by themselves but differ from the expected high-pressure CaSiO₃-perovskite and have not resulted in the approval of CaSiO₃-perovskite as a mineral. We report the discovery of CaSiO₃-perovskite as a mineral approved by the Commission of New Minerals, Nomenclature and Classification (CNMNC) of the International Mineralogical Association (IMA). The new mineral [IMA2020-012a (14)]

is named “davemaoite” in honor of Dave (Hokwang) Mao for his eminent contributions to the field of deep-mantle geophysics and petrology. The type material—inclusions in a diamond from Orapa, Botswana—is deposited in the Natural History Museum Los Angeles (catalog number NHMLA 74541, formerly GRR1507 of the Caltech mineral collection) (15). Davemaoite coexists with orthorhombic carbonaceous α -iron and wüstite (Fe_{0.8}Mg_{0.2})O at 8 to 9 GPa remnant pressure (Fig. 1). Separate inclusions of ilmenite, iron, and ice-VII in the same diamond (16) have remnant pressures of 7 GPa and 8 to 9 GPa, respectively. The x-ray diffraction (XRD) pattern of davemaoite is that of a cubic perovskite (Fig. 1) (15), with, at most, contributions of <5 vol % of material with $\pm 2.5\%$ smaller or larger volume, whereas an overall distortion of the lattice can be excluded on the basis of the reflection intensities (Fig. 1). Cubic ABO₃ perovskites have no internal structural degrees of freedom and comprise only one chemical formula unit. Thus, the identification of this phase is unambiguous even in diffraction patterns with contributions from more than one phase (Fig. 1).

Davemaoite was identified through the XRD pattern of cubic perovskite at a location in the hosting diamond with a CaK α x-ray fluorescence (XRF) signal far above background. Both, XRF and XRD data were obtained at beamline 34-ID-E at the Advanced Photon Source (15). We superimposed the CaK α XRF map (Fig. 2) on a visible light image of the holotype material at the beamline where we subsequently collected the XRF and XRD data. We also made corresponding maps of Fe and Ti (fig. S1). Areas with XRF signal at noise level in Fig. 2 show no x-ray diffraction besides that of diamond. Right after acquisition of the XRF map, we examined by XRD the inclusions that were found by XRF. XRD and XRF were collected on the inclusions when they were fully entrapped in the doubly polished platelet of the hosting diamond. We focused the x-ray beam to an area of 0.5 μ m by 0.5 μ m in order to identify inclusions with high spatial resolution. The inclusions of 4 μ m by 6 μ m and 4 μ m by 16 μ m areas within the red circle of the Ca XRF map corresponded to the XRD patterns of the cubic perovskite (Fig. 1). We added frames with perovskite patterns to obtain better signal and powder statistics.

We confirmed the identification of davemaoite by infrared spectroscopy. Cubic ABO₃ perovskites have no Raman-active modes and three infrared (IR)-active modes (15). We observed two of the three IR-active modes (Fig. 1, inset), while the third one was below the diffraction limit for objects as small as these inclusions. As expected, we observed no Raman peaks (fig. S2). We calculated mode energies by fitting force constants to match *ab initio* calculated zone-center phonon energies of the

¹Department of Geoscience, University of Nevada, Las Vegas, NV 89154, USA. ²National High Magnetic Field Laboratory and Department of Earth, Ocean, and Atmospheric Science, Florida State University, Tallahassee, FL 32310, USA.

³Advanced Photon Source, Argonne National Laboratory, Lemont, IL 60439, USA. ⁴Advanced Light Source, Lawrence Berkeley National Laboratory, Berkeley, CA 94720, USA.

⁵Division of Geological and Planetary Sciences, California Institute of Technology, Pasadena, CA 91105, USA.

*Corresponding author. Email: oliver.tschauner@unlv.edu

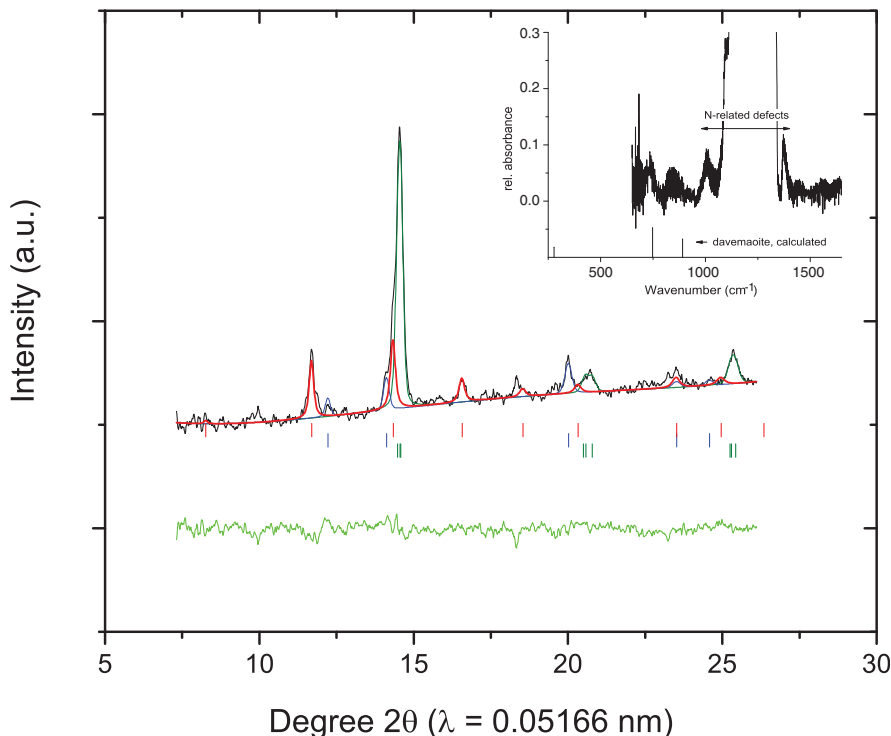


Fig. 1. X-ray diffraction pattern and Rietveld refinement of davemaoite. Davemaoite (dvm), red; (Fe,C), olive; wüstite (wüs), blue; residual of fit, green. Tick marks indicate allowed reflections (same color-coding). The weighted refinement factor, R_{wp} , was 0.046, and the structure-factor moduli-based refinement factor, R_F , for dvm was 0.10. Phase proportions were 35(5), 45(5), and 15(5)% for dvm, (Fe,C), and wüs, respectively. In dvm, the intensity of reflections 100 and 201 indicates sublattice disorder with A-cations shifted from site 1b to the 1/8-occupied site 8g. This is consistent with accommodation of K and Na along with Al and Fe. The paragenesis was found in two inclusions. Volumes of analyzed davemaoite inclusions ranged from 45.1 to 46.3 Å³ [equal to 0 to 6 GPa (7) in pure CaSiO₃], but the actual composition of davemaoite markedly changes the pressure inferred from the volume (9). Coexisting wüstite Fe_{0.8(1)}Mg_{0.2(1)}O has a volume of 74.34(1) Å³, corresponding to 8 to 9 GPa (22). Indications of weak diffraction around dvm peaks near noise level are assigned to minor contributions of material of slightly larger and smaller volume (probably reflecting chemical variation; fit not shown here) but are inconsistent with a tetragonal distortion. a.u., arbitrary units. (Inset) IR spectrum of davemaoite after subtraction of a diamond spectrum collected close to the inclusion. The unprocessed IR spectrum is shown in fig. S3. Bars indicate all calculated IR bands.

tetragonal structure (17) and mapped the tetragonal Brillouin zone onto that of the cubic structure. Intensities are based on the calculated phonon density of state.

Subsequently, we used laser-ablation inductively coupled mass spectrometry (LA-ICP-MS) to excavate and analyze the chemical compositions of two of the inclusions with a 100- μ m-diameter laser beam. We indicate the ablation area with a red circle (Fig. 2). We monitored all mass peaks under medium mass resolution ($m/\Delta m = 4000$), which allowed us to resolve numerous carbon-related molecular interferences on low-mass isotopes. We hit two inclusions of davemaoite at 5 to 8 μ m and 80 to 100 μ m depth below the polished surface (Fig. 2, inset). The time-resolved ⁴⁴Ca signal of the LA-ICP-MS measurement (Fig. 2, inset) shows signal clearly above background level. We also collected equivalent profiles for ⁵⁶Fe, ³⁹K, and ⁵²Cr (fig. S1). In all cases, the signals rose above background at the same depth, consistent with their origin in the same two inclusions. We obtained an average davemaoite composition of (Ca_{0.43(1)}K_{0.20(1)}Na_{0.06}Fe_{0.11(1)}Al_{0.08}Mg_{0.06}Cr_{0.04(2)})(Si_{1.0(2)}Al_{0.00(1)})O₃ (15). We performed a Rietveld refinement (Fig. 1) and provide a crystallographic information file (15).

Next, we describe the hosting diamond and then discuss the pressure-temperature (P-T) conditions of formation of the type davemaoite and its composition. The hosting diamond is different from diamonds that contain potential retrograde products of high-pressure minerals at 0 to 1 GPa remnant pressures (13, 18).

The diamond is of type IaAB with frosted octahedral faces and trigon features (15). We found davemaoite, iron, wüstite, ilmenite, and ice-VII in the center of the diamond. Our analysis of the N-defect IR bands (fig. S3) (12) indicates a low average residence temperature (~1500 K) or a short residence time in the mantle, similar to the holo- and cotype diamonds of ice-VII (18). Short residence time and low average residence temperature are common features of lithospheric diamonds, but in sublithospheric diamonds both parameters act in favor of conserving high remnant pressures and high-pressure minerals by reducing viscoelastic relaxation of the hosting diamond and by preventing retrograde transformations. The bulk modulus of davemaoite depends on its composition (7, 8) and is unknown for the given composition. However, coexisting wüstite is at a remnant pressure of 8 to 9 GPa (16). For a single inclusion of wüstite, this remnant pressure would correspond to an entrapment pressure of ~40 GPa if pressure were to evolve along a purely elastic path (15). However, diamond becomes viscoelastic between 1100 and 1200 K, even at laboratory time scales (19). To account for this nonelastic behavior of the hosting diamond, we use the method of Wang *et al.* (20), which does not rely on initial assumptions about the entrapment temperature and uses the P-T paths of separate inclusions in the same diamond: wüstite, iron, ice-VII, and ilmenite. Using this approach, we assessed entrapment conditions of 29 \pm 5 GPa at 1400 to 1600 K (15). Because visco-

elastic processes are path- and time-dependent, we cannot exclude a higher entrapment pressure or temperature.

We cannot entirely rule out that our chemical analysis is affected by minor contaminants, although we did not observe an XRD signal or a marked XRF signal of any phase other than davemaoite, wüstite, and iron in the excavated region. Furthermore, we note that (i) the low Ti is a result unaffected by potential contamination and (ii) the ³⁹K signal occurs at the same depth as the ⁴⁴Ca signal of davemaoite. We did not observe by XRD alternative hosts of K and Ca such as liebermannite and harmunite-type (Ca,K,Na)(Al,Si)₂O₄ anywhere in this diamond. Both of these phases, and any phase dominated by K and Ca, give diffraction patterns that are very different from the perovskite-type pattern we observed. Hence, we believe the presence of K and Al in davemaoite is not likely the result of a contaminated analysis but rather indicates coupled substitution of a large and a small cation K,Na + Al,Fe for Ca. Generally, a substitution of K for Ca and Al for Si shifts the material into the stability field of ABO₃ perovskites with a trend toward high crystal symmetry (21).

Our result indicates that the postspinel phase (Ca,Na,K)(Al,Si)₂O₄ is not required as a host of Ca, alkalis, and Al in at least the upper region of the lower mantle. It is possible that type davemaoite formed retrograde out of postspinel through a reaction (Ca,Na,K)(Al,Fe³⁺,Si)₂O₄ + Fe⁰ \rightarrow (Ca,Na,K)(Al,Si)O₃ + FeO, but for this process one expects the presence of remnant

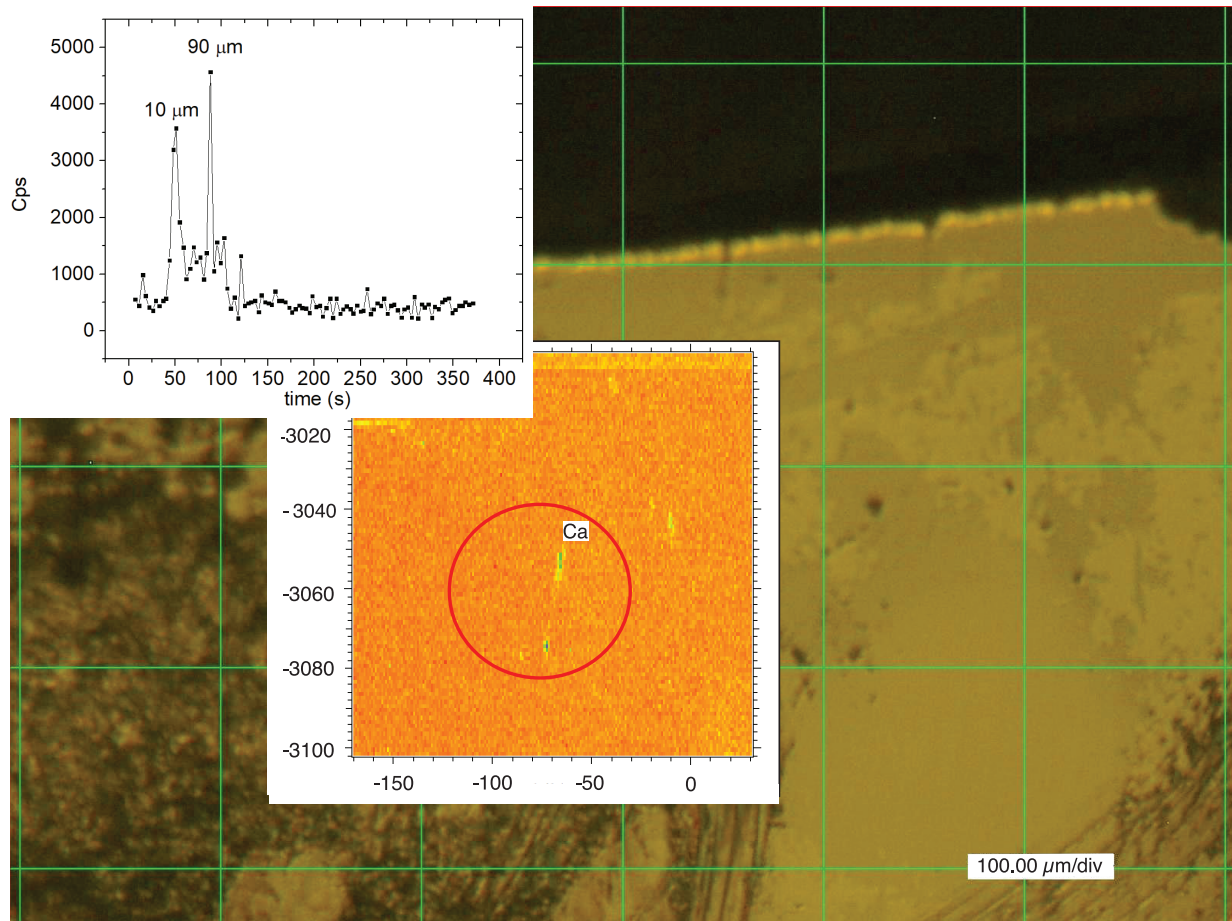


Fig. 2. Reflected light image of the diamond at the beamline. The XRF map of CaK α is superimposed. The x and y axes give the sample coordinates in micrometers. The red circle indicates the area ablated during LA-ICP-MS analysis. The two Ca-rich areas in the circle correspond to diffraction patterns of davemaoite. The more intense signal around $x,y = 72,-3074$ corresponds to

the shallow inclusion at 8 to 10 μm depth. Depth was assessed from the attenuation of the XRF signal of Ca and Fe and from the depth of the pit after ablation. (Inset) Time-resolved ^{44}Ca signal of LA-ICP-MS measurement. Ablation started at time (t) = 48 s and finished at 108 s. Cps, counts per second; div, divisions of the grid.

postspinel in the paragenesis, which is not observed. In the deep mantle, davemaoite takes on a role similar to that of garnet in the upper mantle. Both minerals have a “garbage can” crystal chemistry that allows them to host many elements that are incompatible in upper-mantle minerals (6, 7). Our observations are fully consistent with the experimental results that this mineral dissolves LILEs, specifically K (6, 7). Experimental studies that were based on peridotite and MORB (mid-ocean ridge basalt)-like bulk compositions formed davemaoite with lower K content and higher Ti content than the type material, which is expected for these starting compositions. We argue that the low Ti and high K content of type davemaoite reflects a different, K-rich source composition, possibly resulting from deep-mantle metasomatism, which is also indicated by the presence of ice-VII and by the hosting diamond itself (16). This point emphasizes the importance of studying natural specimens of high-pressure minerals,

because they record a petrologic complexity of deep Earth that may not be assessed in experiments. Depletion of Ti in type davemaoite is a possible result of the presence of phases that strongly partition Ti, such as liuite, FeTiO₃-perovskite. Ilmenite has been observed in the same diamond at similar remnant pressure as the davemaoite-wüstite-iron inclusion, and its P-T path intersects the phase boundary of liuite (15). Hence, our findings indicate that the source rock composition of type davemaoite deviated from peridotite and, thus, that chemical segregation occurs in the lower mantle, possibly down to 900 km according to our estimate (fig. S4). This variation in rock composition affects heat generation through radioactive decay in the lower mantle where davemaoite scavenges K, as shown here, and U and Th, as experimentally shown (7).

REFERENCES AND NOTES

1. F. E. Brenker, F. Nestola, L. Brenker, L. Peruzzo, J. W. Harris, *Am. Mineral.* **106**, 38–43 (2020).

2. O. Tschauner, *Am. Mineral.* **104**, 1701–1731 (2019).
3. L. Liu, A. E. Ringwood, *Earth Planet. Sci. Lett.* **28**, 209–211 (1975).
4. K. Hirose, R. Sinmyo, J. Hernlund, *Science* **358**, 734–738 (2017).
5. S. Gréaux *et al.*, *Nature* **565**, 218–221 (2019).
6. K. Hirose, N. Shimizu, W. van Westrenen, Y. W. Fei, *Phys. Earth Planet. Inter.* **146**, 249–260 (2004).
7. S. Gréaux *et al.*, *Phys. Earth Planet. Inter.* **174**, 254–263 (2009).
8. J. Korenaga, *Rev. Geophys.* **46**, RG2007 (2008).
9. H. W. Chen *et al.*, *Am. Mineral.* **103**, 462–468 (2018).
10. A. M. Glazer, *Acta Crystallogr. A* **31**, 756–762 (1975).
11. O. Tschauner *et al.*, *Science* **346**, 1100–1102 (2014).
12. N. Tomioka, K. Fujino, *Science* **277**, 1084–1086 (1997).
13. F. Nestola *et al.*, *Nature* **555**, 237–241 (2018).
14. R. Miyawaki, F. Hatert, M. Pasero, S. J. Mills, *Eur. J. Mineral.* **32**, 645–651 (2020).
15. Materials and methods are available as supplementary materials.
16. O. Tschauner *et al.*, *Science* **359**, 1136–1139 (2018).
17. R. Caracas, R. Wentzcovitch, G. D. Price, J. Brodholt, *Geophys. Res. Lett.* **32**, L06306 (2005).
18. T. Stachel, G. P. Brey, J. W. Harris, *Elements* **1**, 73–78 (2005).
19. D. J. Weidner, Y. Wang, M. T. Vaughan, *Science* **266**, 419–422 (1994).
20. W. Wang *et al.*, *Innovation* **2**, 100117 (2021).

21. V. M. Goldschmidt, *Naturwissenschaften* **14**, 477–485 (1926).
22. S. D. Jacobsen *et al.*, *J. Synchrotron Radiat.* **12**, 577–583 (2005).
23. O. Tschauner, S. Huang, S. Yang, M. Humayun, W. Liu, S. N. Gilbert Corder, H. A. Bechtel, J. Tischler, G. R. Rossman, Raw data for davemaoite Dryad (2021); <https://doi.org/10.5061/dryad.jq2bvq89m>.

ACKNOWLEDGMENTS

We thank N. Tomioka and an anonymous reviewer for their helpful comments. **Funding:** This work was supported by awards NSF-EAR-1838330, -EAR-1942042, and -EAR-1322082; the NSF Cooperative Agreement No. DMR-1644779; and the State of Florida.

Use of the Advanced Photon Source and the Advanced Light Source were supported by the US Department of Energy, Basic Energy Sciences, contracts DE-AC02-06CH11357 and DE-AC02-05CH11231, respectively. **Author contributions:** O.T., S.H., S.Y., and M.H. participated in design, interpretation, data collection, and analysis of the reported results and in drafting and revising the manuscript. W.L., S.N.G.C., H.A.B., J.T., and G.R.R. participated in data collection and revising the manuscript. **Competing interests:** The authors have no competing interests. **Data and materials availability:** Additional chemical and crystallographic information about davemaoite is provided in the supplementary materials. Raw data are deposited at Dryad (23). Crystallographic and chemical information on type davemaoite is deposited in the Inorganic

Crystal Structure Database. The type material is deposited with the NHMLA under accession number 74541.

SUPPLEMENTARY MATERIALS

science.org/doi/10.1126/science.abl8568
Materials and Methods
Figs. S1 to S4
Tables S1 and S2
References (24–40)
Data S1

9 August 2021; accepted 21 September 2021
[10.1126/science.abl8568](https://doi.org/10.1126/science.abl8568)

Discovery of davemaoite, CaSiO-perovskite, as a mineral from the lower mantle

Oliver Tschauner Shichun Huang Shuying Yang Munir Humayun Wenjun Liu Stephanie N Gilbert Corder Hans A. Bechtel Jon Tischler George R. Rossman

Science, 374 (6569), • DOI: 10.1126/science.abl8568

Lower mantle “garbage can”

Calcium silicate perovskite has finally been identified in a natural sample and now has the mineral name davemaoite. Tschauner *et al.* discovered the type mineral trapped at high pressure and temperature as a diamond inclusion (see the Perspective by Fei). Structural and chemical analysis of the mineral showed that it is able to host a wide variety of elements, not unlike fitting bulky objects into garbage can. Specifically, it has a large amount of trapped potassium. Davemaoite can thus host three of the major heat-producing elements (uranium and thorium were previously shown experimentally) affecting heat generation in Earth’s lower mantle. —BG

View the article online

<https://www.science.org/doi/10.1126/science.abl8568>

Permissions

<https://www.science.org/help/reprints-and-permissions>

Use of this article is subject to the [Terms of service](#)

Science (ISSN) is published by the American Association for the Advancement of Science, 1200 New York Avenue NW, Washington, DC 20005. The title *Science* is a registered trademark of AAAS.

Copyright © 2021 The Authors, some rights reserved; exclusive licensee American Association for the Advancement of Science. No claim to original U.S. Government Works